The Conversion of Cyclohexane to Adipic Acid catalyzed by an Iron-Porphirin Complex. A theoretical study.

Holger Noack*, Valentin Georgiev*, Johannes Adam Johannson**, Margareta R.A. Blomberg*,Per E.M. Siegbahn*

*Department of Physics, Albanova, Department of Biochemistry and Biophysics, Arrhenius Laboratories, Stockholm University, S-106 91, Stockholm, Sweden.
Telephone: +46 8 161268
Fax: +46 8 55378601
E-mail: holger.noack@fysik.su.se

**Department fur Chemie, Universität in Aachen, Aachen, 07345, Germany.
Telephone: +49 0 070815
Fax: +49 0 070815

Running Title: Catalyic Adipic Acid Generation

Keywords: biomimetic complexes, adipic acid, heme, density functional calculations, spin transition, catalysis

1. Introduction.

Adipic acid (IUPAC name hexanedioic acid) is the most important dicarboxylic acid for the industry, with an annual production of about 2.5 billion kg. Its main application is as a precursor for the production of nylon and other polymers (PVC, Polyurethane), and in small quantities it is used as a flavorant, acidulant and gelling aid in baking powders [1]. Since adipic acid occurs rarely in nature, these enormous amounts are synthesized by the chemical industry. Historically, adipic acid was produced by oxidation of various fats, while the contemporary methods are based on oxidation of cyclohexane. First the cyclohexane is oxidized at 150-160° C with oxygen in the presence of homogeneous cobalt or manganese catalyst to a mixture of cyclohexanol and cyclohexanone called "KA oil" (abbreviation of "ketone-alcohol oil). The KA oils can be further oxidized with nitric acid, hydrogen peroxide or molecular oxygen to adipic acid. The use of nitric acid has disadvantages from environmental point of view, but is preferred due the low cost of the nitric acid as oxidant. Hence, there is increasing interest towards usage of molecular oxygen or hydrogen peroxide, which provide far more environmental friendly oxidation.

The so called one-pot oxidation has been reported from different groups [2–4]. The one-pot synthesis is a strategy where a reactant is subjected to successive chemical reactions in just one reactor. This improves the efficiency of a chemical reaction because a lengthy separation process and purification of the intermediates are avoided, while the yields are increased. These methods however, have some disadvantages that still make the process expensive – use of expensive radical catalyst, acidic solvent, severe reaction conditions. Utilizing of metalloporphyrins as catalysts for the one-pot synthesis of adipic acid from cyclohexane and molecular oxygen has been reported [5, 6] as promising, but up to date it is still hard to be applied in industry due to low yields.

Porphyrin-iron complexes (hemes) are well known tightly-bound cofactors (prosthetic groups) in a number of metalloproteins – Hemoglobin, Cytochrome C, P450, Peroxidases, etc. The biological functions that they are involved in include dioxygen transportation, electron transfer, redox chemistry. The heme enzymes and synthetic complexes require an additional cofactor (for example Cysteine in P450) in order to active the O_2 molecule for substrate oxidation. Two Porphyrin-iron complexes however can bind dioxygen as a peroxide in a di-iron complex and cleave the O-O bond, as reported by Chin and co-workers [7]. The O-O bond cleavage in binuclear Porphyrin peroxo complexes was recently studied theoretically [8] with DFT. The stability of the binuclear center at normal temperature was explained with the splittings of the spin states and the way they are changed in the presence of axial ligands.

In the present contribution, the stepwise mechanism of the catalytic oxidation of cyclohex-

ane to adipic acid was investigated theoretically. Hybrid density functional theory (DFT) was used to model the putative oxidative stages in the adipic acid synthesis. The reaction was modelled according to the conditions reported in ref. [6] – solvent-free reaction system with molecular oxygen as the only oxidant, and a heme iron-oxo complex (PorfFe(IV)=O) as a catalyst, at 413K temperature.

The suggested mechanism consists of three major oxidative steps: (i) oxidation of cyclo-

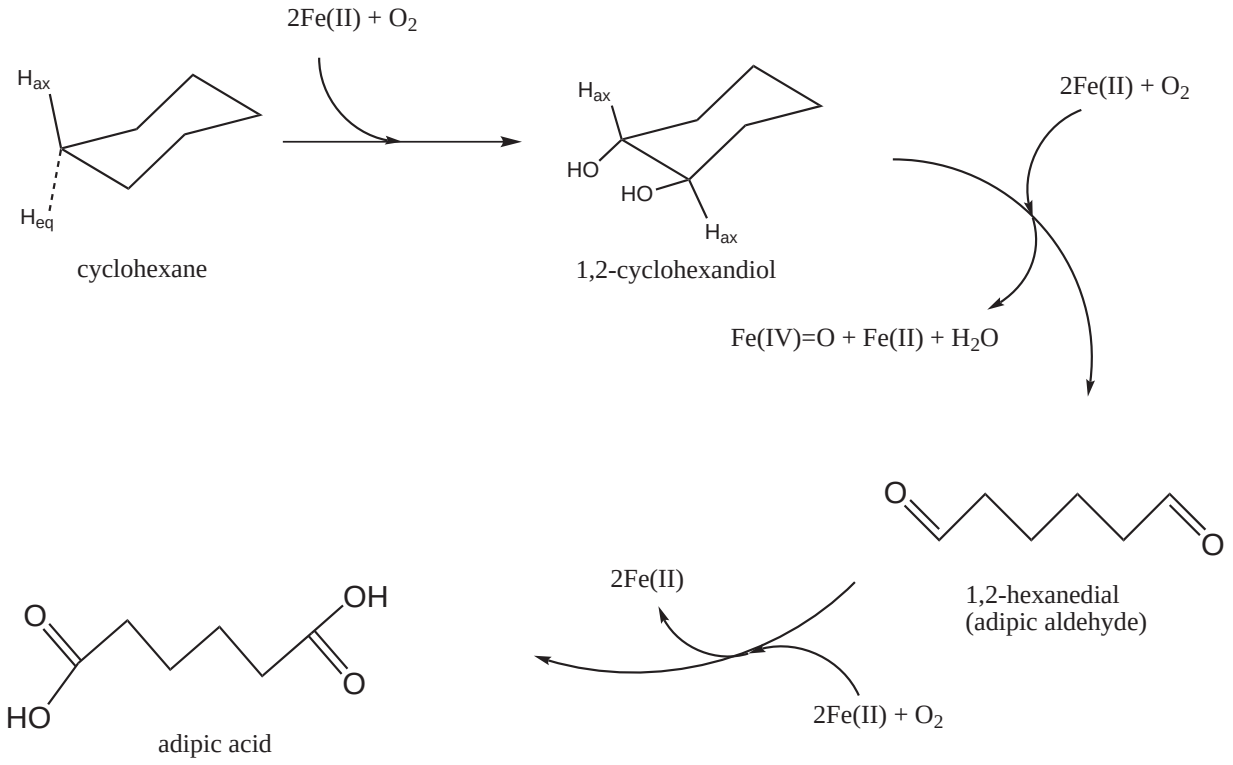

Scheme 1: The main oxidative steps in the suggested mechanism for direct synthesis of adipic acid from cyclohexane.

hexane to 1,2-cyclohexanediol by molecular oxygen, (ii) oxidation and ring opening of the 1,2-cyclohexanediol to 1,6-hexanedial (adipic aldehyde), (iii) final oxidation of the adipic aldehyde to adipic acid (see Scheme 1).

2. Computational details.

Geometry optimizations were performed using the hybrid density functional B3LYP [9] [10] [11] [12] [13], for which the exchange part is a combination of the gradient corrected LDA exchange with 20% Hartree-Fock exchange. While B3LYP is known to be reliable for the prediction geometries of transition metal complexes, it has been reported that acti-

vation energies and the energetic separation of spin states is better described by reducing the amount of Hartree-Fock exchange from 20% to 15% [14]. For this reason, single-point calculations using 15% Hartree-Fock exchange, were performed on the B3LYP geometries. The effects of varying the amount of Hartree-Fock exchange will be discussed below.

The software package Jaguar 5.5/7.0 [15] was used for geometry optimizations and for the calculation of the final energies. Geometry optimizations were performed using the double zeta basis set lacvp. This basis set is composed of the 6-31G description for all light atoms and an effective core potential (ECP) on iron [16]. The final energies for the fully optimized structures were calculated at higher level of theory. The correlation-consistent polarized basis set cc-pVTZ(-f) (without f-functions) was used for all atoms except iron. This triple zeta quality basis set, which is intrinsically polarized does not include an ECP, therefore lacv3p** basis set was explicitly used for iron. Experience has shown, that geometries obtained from calculations using the double zeta basis are quite adequate for the calculation of the final energetics [17] [18].

In order to take into account the polarization effects of the solvent used in the experiments, the self-consistent reaction field (SCRF) method implemented in Jaguar was employed [19] [20]. In this case the cyclohexane itself act as solvent and provides the reaction environment, hence the dielectric constant of 2.0 (corresponding to cyclohexane) was used. In the SCRF method the system is described as a solute contained in a cavity inside a polarizable dielectric continuum. Final energies of the optimized structures were corrected for the solvent effects by employing the lacvp basis set. Normally the dielectric medium has a very small effect on the reaction energetics as long as no substantial charge separations are involved [21] [22]. This is very well manifested in the present case, where the total charge of the model is zero. All the calculated solvent solvent effects were smaller than 4 kcal/mol. Reported spin populations indicate the spin and oxidation state of the metal ion and were derived from Mulliken population analysis.

Hessian matrices (i.e. matrices of harmonic force constants) were calculated with the small basis, lacvp, using Gaussian 03 [23]. The vibrational eigenvalues derived from the Hessians, were used to verify the nature of the optimized stationary points, i.e. local minima (having no imaginary frequencies) and transition states (having one imaginary frequency). The Hessians were also used for the evaluation of zero point vibrational effects, entropic and thermal corrections to the Gibbs free energy.

Although the partition functions for an ideal gas are very accurate for predicting gas phase entropies, errors are introduced when this method is applied to solvent molecules. In particular, the calculated gas phase entropy of the cyclohexane molecule is higher than the entropy it has in the liquid phase. In principle, it is possible to estimate the difference by using experimentally determined entropies, and for cyclohexane it corresponds to the

measured vaporization enthalpy of 9.3 kcal/mol at T=413K [24, 25]. This number is very close to the calculated entropy lost of 8.3 kcal/mol (at T=413K) for the transition state for hydrogen atom transfer from cyclohexane to Fe(IV)-oxo. In the later reaction steps molecules very similar to the cyclohexane form complexes and react with the heme complex, but they should be present in low concentrations in the solution and the entropy loss associated with complex formation should thus be larger than for cyclohexane. At present, we are not certain about the accuracy of the calculated entropy affects, therefore the relative enthalpies was used in the energy profiles.
To account for the Van der Waals forces additional calculations were done with B3LYP-D using the Orca Package [27, 28]. Corrections of 3-4 kcal/mol were calculated for these long-range dispersion interactions, but their effect on the relative energies was found to be very small, in the range of 0.5 to 1.0 kcal/mol.
The complex used as a catalyst in the experiment is *meso*-Tetra(*o*-chlorophenyl)iron Porphyrin (T(*o*-Cl)PPFe). An unsubstituted Porphyrin ligand was used in the calculations. This strategy for decreasing the computational costs has been proven to give adequate results in recent theoretical study where the energetical differences between substituted and unsubstituted Porphyrin models were found insignificant.

3. Results and discussion.

The oxidation of cyclohexane to adipic acid by the biomimetic heme complex T(*o*-Cl)PP-Fe^{IV}(O) was studied using Density Functional Theory. Experimentally the reaction was done with the cyclohexane itself being a solvent, and with molecular oxygen as the only oxidant. The model reaction starts from a loose complex between the iron-oxo species (Porph)Fe^{IV}=O and the cyclohexane. The suggested mechanism consists of three major steps. In the first one the cyclohexane is hydroxylated to 1,2-cyclohexanediol

Oxidation of cyclohexane to 1,2-cyclohexanediol.

The ground state of the reactant complex (Figure 2 **A**) is a triplet having formally two unpaired electrons on iron, of which one is partially delocalized to the oxo group (S_{Fe}=1.21 and S_{oxo}=0.83, where S_X refers to the Mulliken population spin density of fragment $_X$).

In the ground state of the reactant complex, there are two possible electronic mechanisms for the hydrogen atom transfer (HAT) from the substrate to the oxo group of [(Porph)Fe^{IV}(O)]. If the transfered H-atom carries an α-spin, the spin on iron increases (defining the spin on iron as α). This type of mechanism yields an intermediate complex [(Porph)Fe^{III}(OH)(C_6H_{11})$^\bullet$], in which iron has three unpaired electrons that are antiferro-

magnetically (AFM) coupled to the unpaired electron on the substrate radical. The free energy barrier for HAT leading to the AFM triplet state is 21.5 kcal/mol (see Figure 3). If

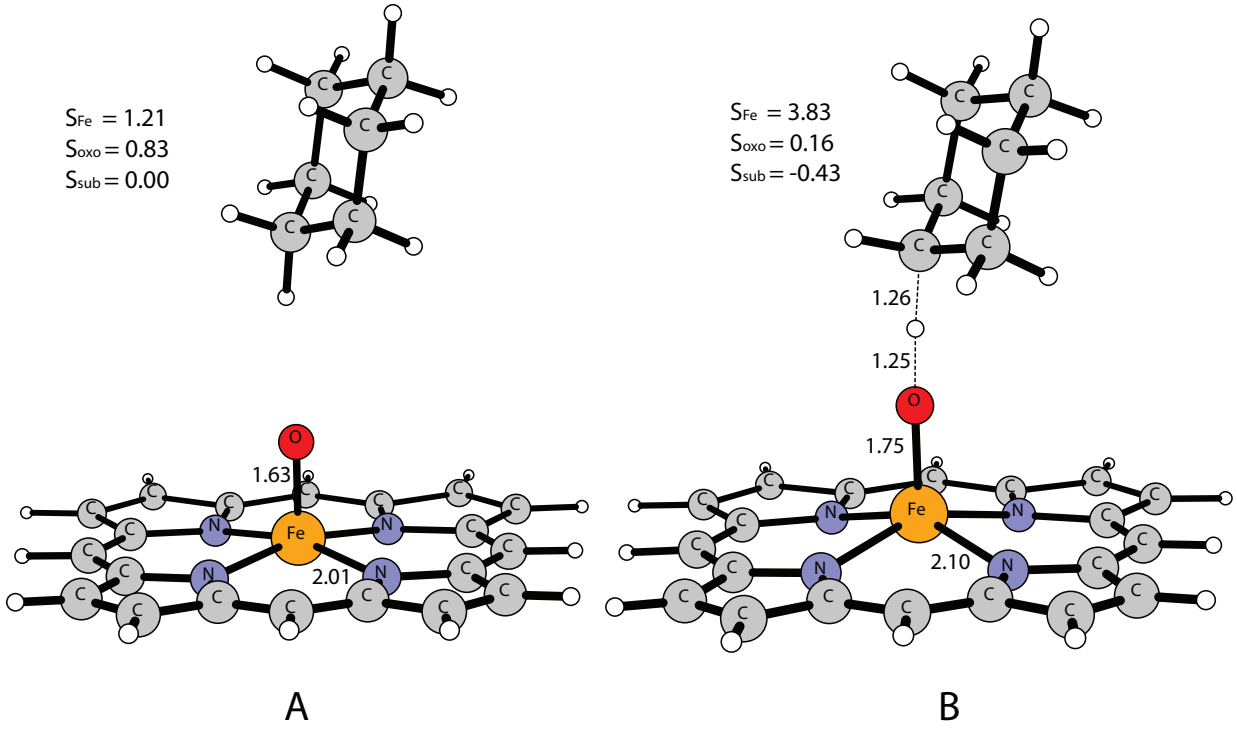

Figure 2: Optimized structures of **A**: the reactant complex [(Porph)Fe^{IV}(O)(C$_6$H$_{12}$)] in its ground triplet state; **B**: HAT transition state in AFM quintet state. The most important distances and spin populations are given.

the transferred H-atom instead carries a β-spin (once again defining the spin on iron as α), the spin on iron decreases when the incoming electron pairs up with one of the its unpaired electron. This type of electronic mechanism yields a complex [(Porph)Fe^{III}(OH)(C$_6$H$_{11}$)$^{\bullet}$], in which one unpaired electron on iron is ferromagnetically (FM) coupled to the unpaired electron on the substrate radical. The enthalpy barrier for this ^{3}HAT$_{FM}$ is 19.8 kcal/mol, i.e. 2.6 kcal/mol higher than for the ^{3}HAT$_{AFM}$ triplet state.

Despite the fact that the ground state of the reactant complex [(Porph)Fe^{III}(O)(C$_6$H$_{12}$)] is a triplet, the lowest barrier for HAT is not found in any of the triplet states, but in the quintet state. In the reactant complex, the quintet state is 7.8 kcal/mol higher than the triplet ground state. But typically for the iron(IV)oxo group, the system undergoes a spin crossing before the transition state is reached. In the TS for hydrogen atom transfer the quintet state (Figure 2 **B**) is 3.6 kcal/mol lower than the TS in the AFM triplet state. The free energy barrier determined by the TS in the quintet state is thus 13.6 kcal/mol with respect to the starting complex [(Porph)Fe^{III}(O)(C$_6$H$_{12}$)] in its triplet ground state. The

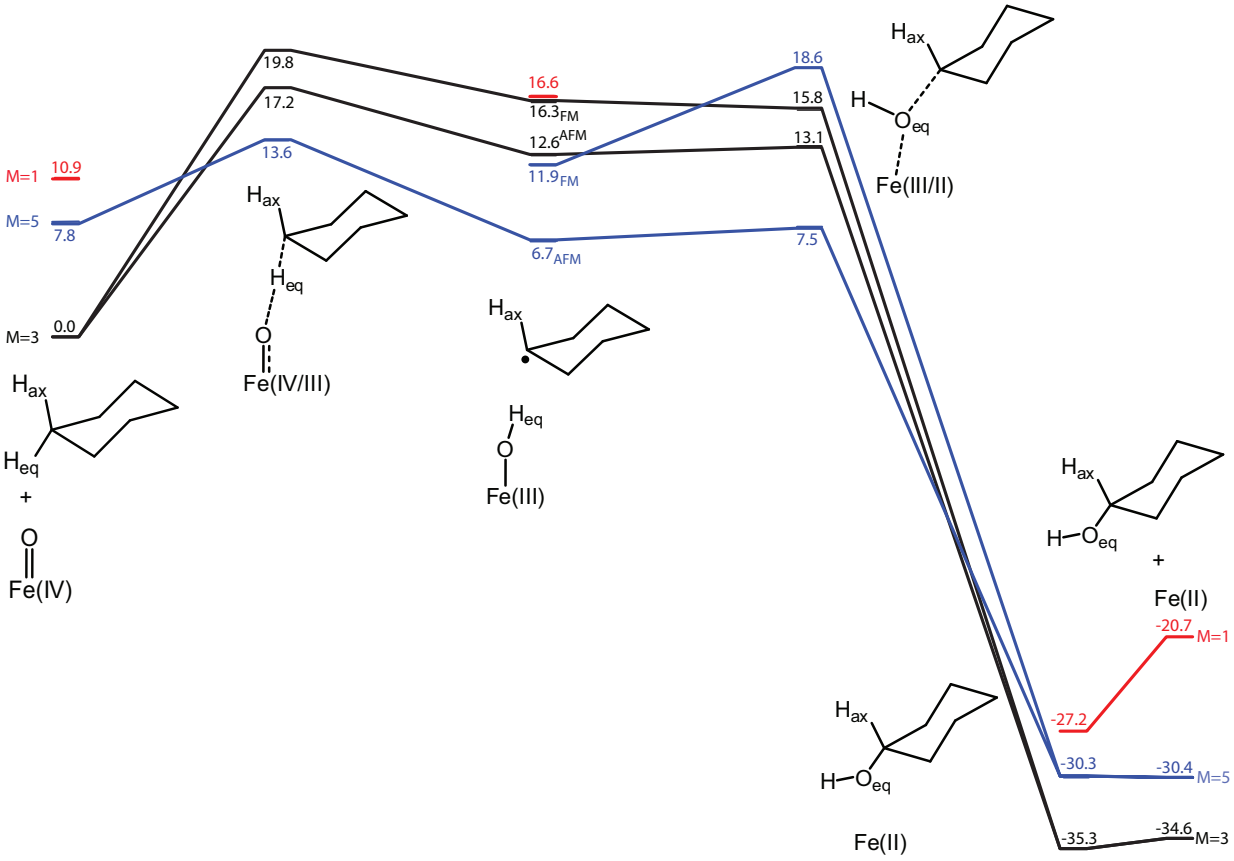

Figure 3: Energy diagram for the first HAT and OH rebound, resulting in the formation of cyclohexanol.

HAT is endergonic with 6.7 kcal/mol.

In the intermediate complex [(Porph)Fe^{III}(OH)(C$_6$H$_{11}$)$^\bullet$], iron has formally been reduced from iron(IV) to iron(III). The ground state of the intermediate is now a quintet, in which iron has formally five unpaired electrons (S$_{Fe}$=4.00, S$_{OH}$=0.39) AFM coupled to the unpaired electron on the substrate radical. The FM coupled quintet state, having formally three unpaired electrons (S$_{Fe}$=2.58, S$_{OH}$=0.44), which are parallel with the unpaired electron on the substrate radical, is found 5.2 kcal/mol higher than the AFM quintet. The AFM and FM triplets are respectively 5.9 and 9.6 kcal/mol higher than the quintet ground state in the intermediate complex [(Porph)Fe^{III}(OH)(C$_6$H$_{11}$)$^\bullet$].

The free energy for the formation of the closed-shell product cyclohexanol is -42.0 kcal/mol and barrier for this process is expected to be very low. The optimized TS is 0.7 kcal/mol above the preceding intermediate complex [(Porph)Fe^{III}(OH)(C$_6$H$_{11}$)$^\bullet$]. The barriers in the higher states are 6.4, 9.1, and 11.9 kcal/mol, for the AFM triplet, the FM triplet, and the FM quintet, respectively. In the reactive quintet state the second step is ex-

ergonic by 37.0 kcal/mol. However, before the product complex [(Porph)$Fe^{II}(C_6H_{11}(OH))$] is reached, a second spin crossing occurs and the ground state of the product complex is the triplet state. The product complex is in close equilibrium with the free species (ΔG=-0.7 kcal/mol).

During the whole reaction, the open-shell singlet state lies higher than the other states. The singlet radical intermediate [(Porph)$Fe^{III}(OH)(C_6H_{11})^{\bullet}$] in particular, was found to lie 9.9 kcal/mol above the ground quintet state. Therefore it was concluded that the singlet state is not involved in the reaction and transition states were not located for this spin state.

It should be noted here that the cyclohexane molecule is in its lowest-energy *chair* conformation, where **axial** and **equatorial** positions can be distinguished. The hydroxylation of the cyclohexane, described above, occurs at an equatorial position.
The second hydroxylation starts with new [(Porph)$Fe^{IV}(O)$] reactant, which forms a weak hydrogen-bonded complex (binding enthalpy -8.3 kcal/mol) with OH-group of cyclohexanol $C_6H_{11}(OH)$(Figure 5**A**). The spin splitting for this reactant is similar to first one - triplet ground state (S_{Fe}=1.28 and S_{oxo}=0.78), quintet state lying 7.7 kcal/mol higher, and singled at 9.5 kcal/mol (Figure 4).

The hydrogen atom that is abstracted in this stage is sitting at ortho-equatorial position, relative to the OH-group of the cyclohexanol. The same electronic aspects of the HAT mechanism can be considered, as in the first oxidation. Two possible radical intermediates [(Porph)$Fe^{III}(OH)(C_6H_{10}OH)^{\bullet}$], AFM- and FM-coupled, arise from both the triplet and the quintet reactants. The enthalpy barrier for formation of the AFM triplet is 20.8 kcal/mol, while for the AFM quintet it is 3.0 kcal/mol lower, and is the lowest found (Figure 5**B**). It is seen that again a spin crossing to the quintet state occurs before the HAT transition state. A transition state for the FM quintet was located and optimized, but it lies 27.8 kcal/mol above the ground state reactant.

The HAT process in endergonic with 8.6 kcal/mol and the ground state of the resulting intermediate [(Porph)$Fe^{III}(OH)(C_6H_{10}OH)^{\bullet}$] is an AFM quintet ($S_{Fe}$=4.03, S_{OH}=0.32). The FM coupled quintet state (S_{Fe}=2.65, S_{OH}=0.35) is found 3.4 kcal/mol higher than the AFM quintet. The AFM and FM triplets are respectively 3.2 and 8.3 kcal/mol higher than the quintet ground state in the intermediate complex [(Porph)$Fe^{III}(OH)(C_6H_{10}OH)^{\bullet}$].

The hydroxylation of the radical proceeds on the AFM quintet surface, but the ground state for the product [(Porph)$Fe^{II}(C_6H_{10}(OH)_2)$] is again the triplet. The lowest optimized TS (AFM quintet) is 3.1 kcal/mol above the preceding intermediate, and the AFM triplet transition state is 8.6 kcal/mol. The free energy for the formation of the product 1,2-

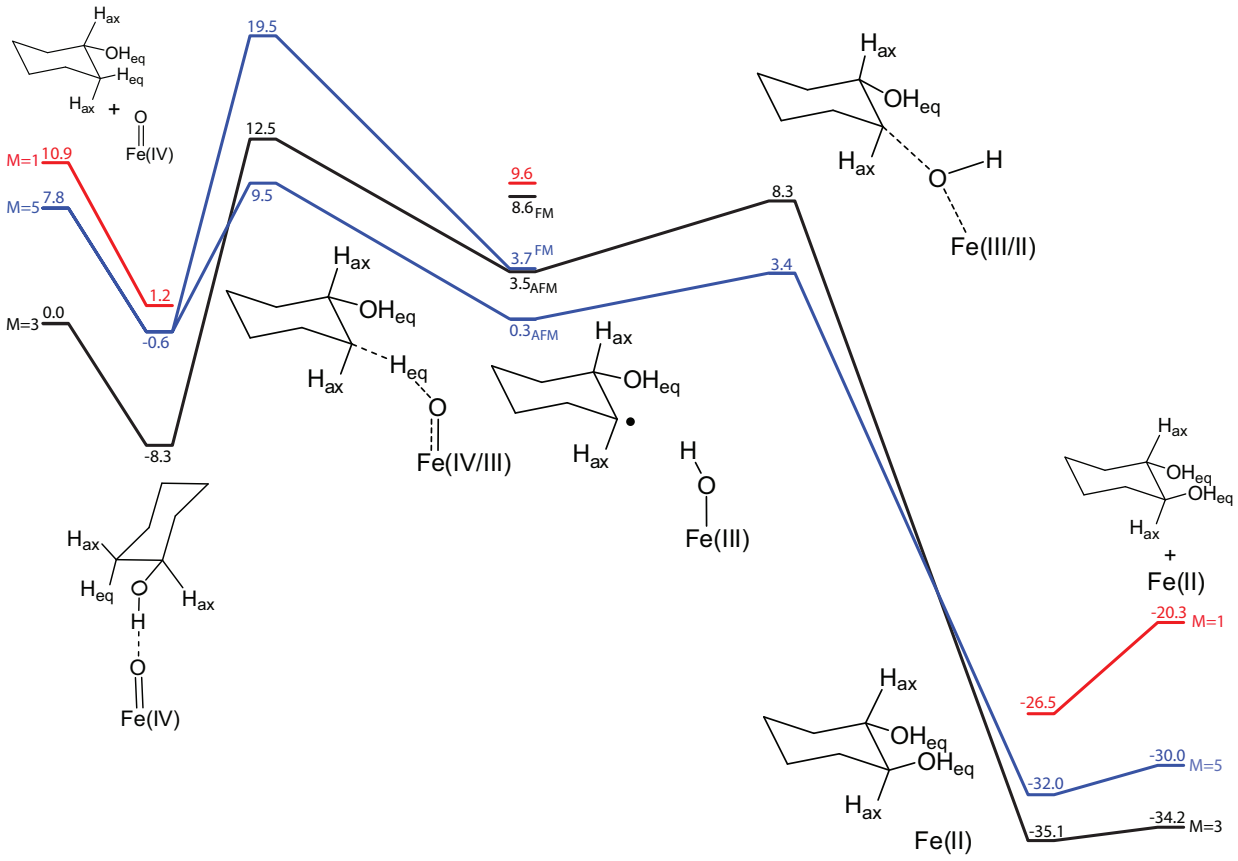

Figure 4: Energy diagram for the second hydroxylation.

cyclohexanediol is -35.4 kcal/mol, determined by the energy of the ground triplet state. The quintet and singlet states of the product are 2.9 and 8.6 kcal/mol higher, respectively, than the ground state. The resulting 1,2-cyclohexanediol has its two OH-groups at neighboring equatorial positions $(C_6H_{10}(OH)_2)_{eqeq}$ of the ring. Two other conformations are possible for ortho-substitution – one of the groups in equatorial, and the other one in axial position $(C_6H_{10}(OH)_2)_{eqax}$, and both groups in axial positions $(C_6H_{10}(OH)_2)_{axax}$. The di-equatorial conformation was found to form the most stable complex with [(Porph)Fe^{IV}(O)], which is the starting reactant for the next major step – the oxidation of 1,2-cyclohexanediol to 1,6-hexanedial (adipic aldehyde).

1,2-cyclohexanediol oxidation and ring cleavage.

The oxo group of [(Porph)Fe^{IV}(O)], forms a weakly (ΔG=-4.0 kcal/mol) hydrogen bonded complex [(Porph)Fe^{IV}(O)($C_6H_{10}(OH)_2$)] with the two OH groups of 1,2-cyclohexanediol ($C_6H_10(OH)_2$). The ground state of the reactant complex (Figure 7 **A**) is a triplet S_{Fe}=1.42 and S_{oxo}=0.65, with the quintet and the singlet at 5.8 and 9.9 kcal/mol, respectively (see Figure 6).

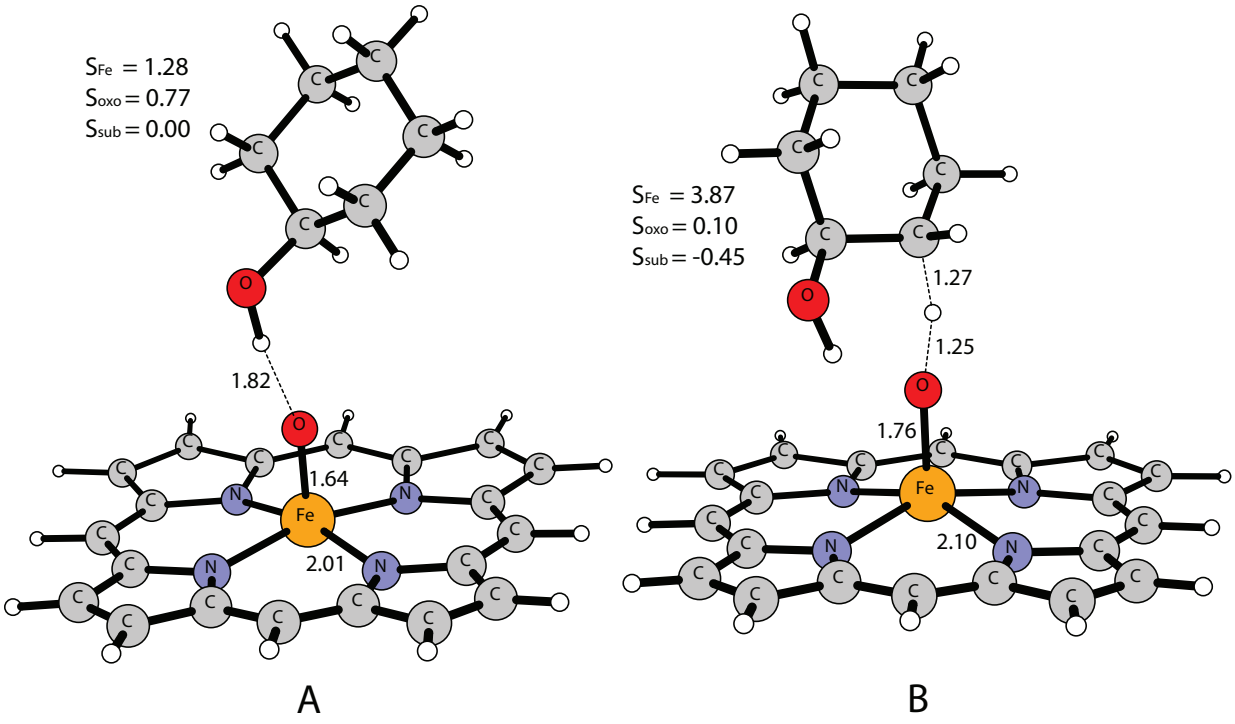

Figure 5: Optimized structures of **A**: the reactant complex [(Porph)Fe(IV)(O)($C_6H_{11}OH$)] in its ground triplet state; **B**: HAT transition state in AFM quintet state. The most important distances and spin populations are given.

First a hydrogen atom is transferred (HAT) from one of the OH groups of the substrate to the oxo group of [(Porph)Fe^{IV}(O)]. This yields a H-bonded intermediate complex [(Porph)Fe^{III}(OH)(C_6H_{10}(OH)$O^{\bullet}$)] (see Figure 7 **C**), whose ground state is a quintet with three unpaired electrons on iron, antiferromegnatically (AFM) coupled to the unpaired electron on the substrate radical. The AFM triplet and the FM quintet states are quite close, at 4.6 and 5.0 kcal/mol above the ground state, respectively. They both have intermediate spin Fe^{III} with three unpaired electrons, that are differently coupled with the unpaired electron on the substrate. In a similar way the FM triplet and the singlet have identical electronic structure of iron and different coupling with the substrate's electron. They lie even higher, at 10.8 and 11.1 kcal/mol, respectively, above the ground state. The spin splitting for the HAT transition state basically follows the one of the resulting intermediate (see Figure 6). The AFM quintet (Figure 7 **B**) determines the lowest path with free energy barrier of 10.2 kcal/mol.

The intermediate complex, in which the substrate is in a radical state, is highly unstable with respect to formation of the closed-shell product 1,6-hexane-aldehyde. The free energy for this step is -39.7 kcal/mol and consequently the barrier is very low. The electronic

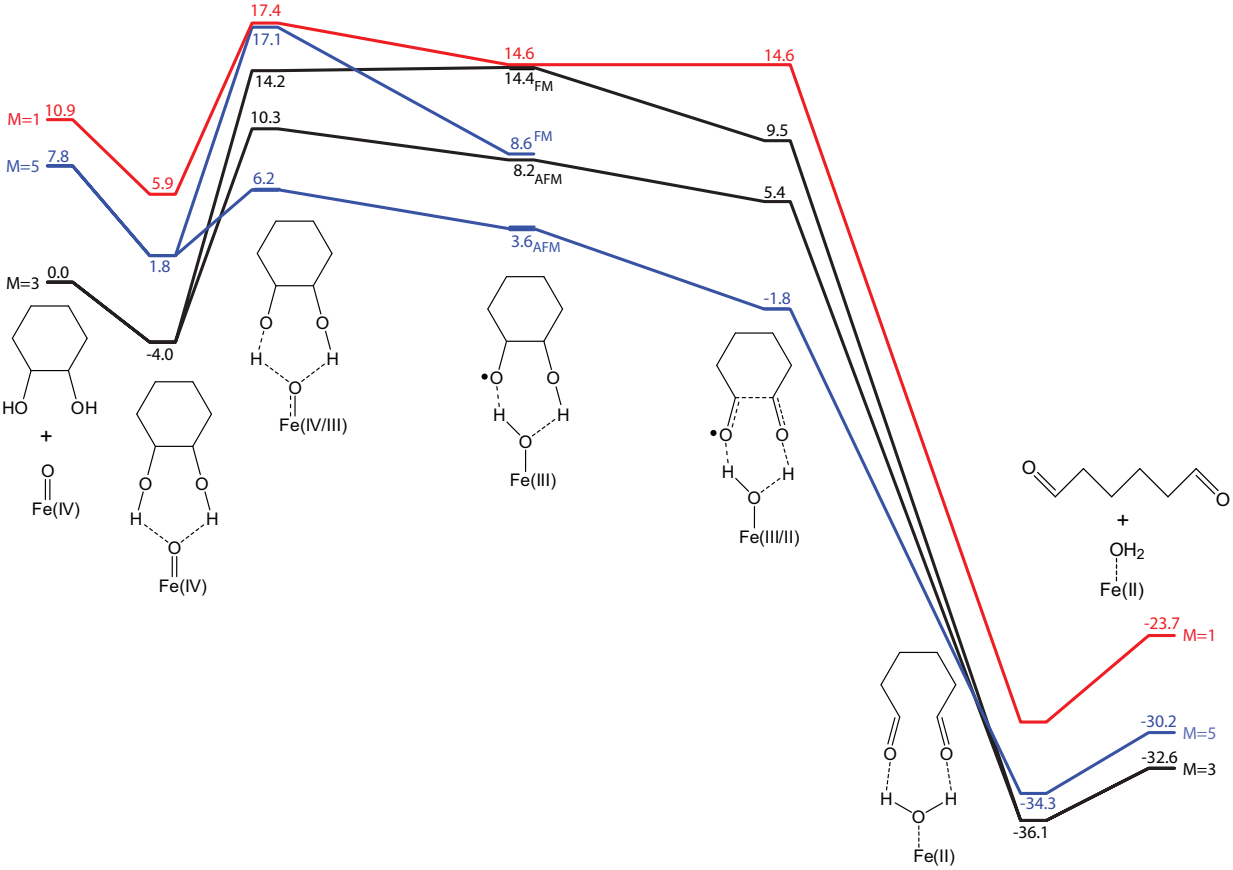

Figure 6: Energy diagram for the two HAT and ring opening of the 1,2-cyclohexanediol ring.

energy barrier for this step in the gas phase is only 3.5 kcal/mol. When the dielectric solvent effects and thermal corrections are added, the energy of the optimized TS becomes 5.4 kcal/mol lower than the preceding intermediate complex [(Porph)Fe^{III}(OH)(C_6OHO$^{\bullet}$)]. The transition state for C-C bond dissociation is concerted with the HAT from the second OH group on the substrate radical to the OH group on iron, see Figure 7 **D**. A sequential process was also considered. It is not possible that the C-C bond dissociates before the second HAT since this requires that the substrate enters a di-radical state. Both the triplet and open-shell singlet states of this di-radical are very high in energy (ca 40 kcal/mol higher than the doublet state of the mono radical in the intermediate complex). In all attempts to find a TS for the second HAT, the C-C bond dissociates with the OH bond. The barriers in the higher states are also found to be very small in magnitude (1.4-7.3 kcal/mol depending on the spin state). It can thus be said that the first HAT is close to concerted with the C-C bond dissociation, and the second HAT. In the reactive quintet state the second step is exergonic by 37.9 kcal/mol. However, before the H-bonded product

complex [(Porph)$Fe^{II}(OH_2)(OHCC_4H_8CHO)$] is reached, a second spin crossing occurs and the ground state of the product complex is the triplet state. The H-bonded product complex is in close equilibrium with the free species (ΔG=-3.5 kcal/mol).

During the whole reaction, the closed-shell singlet state lies up to 5.1 kcal/mol higher than the next highest state. The closed-shell singlet state is thus not involved in the reaction.

Oxidation of adipic aldehyde to adipic acid.

The last major stage consists of two consecutive oxidations of the carbonyl groups of the adipic aldehyde to carboxylic groups. Essentially, each oxidations is again a hydrogen atom transfer followed by a rebound of the OH group. The chemical steps have the same features as in the first two major steps: triplet ground state for the reactant and product; spin crossing before the HAT transition state and after the OH rebound; AFM quintet reactive state.

The reactant is a loose complex between the oxidant [(Porph)Fe^{IV}(O)] and the acyclic adipic aldehyde with binding enthalpy -0.7 kcal/mol (Figure 10 **A**). In the first step a carbonyl hydrogen atom is transfered from one of the carbonyl groups of the substrate to the oxo group of the metal complex. On the reactive AFM quintet PES the calculated activation barrier is 7.7 kcal/mol, and the reaction is exergonic with 7.1 kcal/mol. The following OH group back-transfer goes through an activation barrier of 3.2 kcal/mol and the exergonicity (determined from the triplet ground state of the product) is 50.2 kcal/mol (see Figure 8).

In the very last HAT the activation barriers for the AFM quintet and AFM triplet spin states for the HAT transition state differ by only 0.8 kcal/mol (see Figure 9). Still the quintet should be considered as a reactive state with activation barrier of 8.2 kcal/mol. Optimized geometries for the reactant and the HAT transition state are shown in Figure 11. The resulting radical intermediate lies 3.6 kcal/mol below the ground state reactant, and it takes 1.8 kcal/mol for the iron bound OH group to be rebound. With exergonicity of 51.2 kcal/mol (triplet ground state) the adipic acid is formed.

4. Conclusions.

The catalytic formation of adipic acid from cyclohexane and dioxygen is a strongly exergonic process. Almost each of the sequential steps presented here consists of hydrogen abstraction and hydroxide rebound. The exception is the ring cleavage step where two sub-sequential hydrogen abstractions occur. However, in all of these cases hydrogen abstraction is rate

limiting, with the overall rate limiting HAT involved in hydroxylation of cyclohexanol to ortho-cyclohexanediol. The calculated enthalpy of activation for this step is 17.8 kcal/mol, where the entropy effect is not expected to increase this number significantly. This barrier seems rather high, however, regarding the prevalent reaction conditions a barrier of 24 kcal/mol would correspond to a rate of 1 s^{-1}. The reason that this particular HAT becomes rate limiting can be found in the formation of a rather stable cyclohexanol-Fe(porph) adduct prior to the HAT. This step is furthermore crucial in differentiating between competing reactions, that might lead to the formation of meta- or para-cyclohexanediol, which in turn would lead to different final products. These alternative paths have not been considered in this work, and the challenge to explore them remains. The presented mechanism shows, however, that the underlying chemistry in itself is rather basic.

References

[1] Davis, D. D.; Kemp, D. R. In *Kirk-Othmer Encyclopedia of Chemical Technology*, 4th ed.; Kroscwitz, J. I., Howe-Grant, M., Eds.; Wiley: New York, **1991**; *1*, 466-493.

[2] Iwahama, T.; Syojyo, K.; Sakaguchi, S.; Ishii, Y. *Org. Process Res. DeV.* **1998**, *2*, 255-260.

[3] Pigamo, A.; Besson, M.; Blanc, B.; Gallezot, P.; Blackburn, A.; Kozynchenko, O.; Tennison, S.; Crezee, E.; Kapteijn, F. *Carbon* **2002**, *40*, 1267-1278.

[4] Raja, R.; Thomas, J. M. *J. Mol. Catal. A: Chem.* **2002**, *181*, 3-14.

[5] Ratnasamy, P.; Raja, R. EP 0784045-A1, **1997**.

[6] Ying Yuan, Hongbing Ji, Yixia Chen, Yong Han, Xufeng Song, Yuanbin She, and Rugang Zhong *Org. Proc. Res. Dev.* **2004**, *8(3)*, 418-420.

[7] Chin, D.-H.; Del Gaudio, J.; La Mar, G. N.; Balch, A. L. *J. Am. Chem. Soc.* **1977**, *99*, 5486-5488.

[8] Margareta R. A. Blomberg, Adam Johannes Johansson, and Per E. M. Siegbahn *Inorg. Chem.* **2007**, *46*, 7992-7997.

[9] Lee, C.; Yang, W.; Parr, R. G. *Phys. Rev. B* **1988**, *37*, 785.

[10] Becke, A. D. *J. Chem. Phys.* **1992**, *96*, 2155.

[11] Becke, A. D. *J. Chem. Phys.* **1992**, *97*, 9173.

[12] Becke, A. D. *J. Chem. Phys.* **1993**, *98*, 5648.

[13] Stephens, P. J.; Devlin, F. J.; Chabalowski, C. F.; Frisch, M. J. *J. Phys. Chem.* **1994**, *98*, 11623.

[14] Reiher, M.; Salomon, O.; Hess, B.A. *Theor. Chem. Acc.* **2001**, *107*, 48.

[15] Jaguar 5.5, Jaguar 7.0; Schrödinger, Inc., Portland, Oregon, **2007**.

[16] Hay, P. J.; Wadt, W. R. *J. Chem. Phys.* **1985**, *82*, 299.

[17] Siegbahn, P. E. M. in *Advances in Chemical Physics: New Methods in Computational Quantum Mechanics*, Prigogine, I.; Rice, S. A.; Eds. (1996), John Wiley & Sons, London.

[18] Chong, D. P., Ed. *Recent advances in density functional methods, part II,* **1997**, World Scientific, Singapore.

[19] Tannor, D. J.; Marten, B.; Murphy, R.; Friesner, R. A.; Sitkoff, D.; Nicholls, A.; Honig, B.; Ringnalda, M.; Goddard, W. A. *J. Am. Chem. Soc.* **1994**, *116*, 11875.

[20] Marten, B.; Kim, K.; Cortis, C.; Friesner, R. A.; Murphy, R. B.; Ringnalda, M. N.; Sitkoff, D.; Honig, B. *J. Phys. Chem.* **1996**, *100*, 11775.

[21] Siegbahn, P. E. M.; Blomberg, M. R. A. *Chem. Rev.* **2000**, *100*, 421.

[22] Siegbahn, P. E. M. *J. Comput. Chem.* **2001**, *22*, 1634.

[23] Gaussian 03, Revision D.01,M. J. Frisch, G. W. Trucks, H. B. Schlegel, G. E. Scuseria, M. A. Robb, J. R. Cheeseman, J. A. Montgomery, Jr., T. Vreven, K. N. Kudin, J. C. Burant, J. M. Millam, S. S. Iyengar, J. Tomasi, V. Barone, B. Mennucci, M. Cossi, G. Scalmani, N. Rega, G. A. Petersson, H. Nakatsuji, M. Hada, M. Ehara, K. Toyota, R. Fukuda, J. Hasegawa, M. Ishida, T. Nakajima, Y. Honda, O. Kitao, H. Nakai, M. Klene, X. Li, J. E. Knox, H. P. Hratchian, J. B. Cross, V. Bakken, C. Adamo, J. Jaramillo, R. Gomperts, R. E. Stratmann, O. Yazyev, A. J. Austin, R. Cammi, C. Pomelli, J. W. Ochterski, P. Y. Ayala, K. Morokuma, G. A. Voth, P. Salvador, J. J. Dannenberg, V. G. Zakrzewski, S. Dapprich, A. D. Daniels, M. C. Strain, O. Farkas, D. K. Malick, A. D. Rabuck, K. Raghavachari, J. B. Foresman, J. V. Ortiz, Q. Cui, A. G. Baboul, S. Clifford, J. Cioslowski, B. B. Stefanov, G. Liu, A. Liashenko, P. Piskorz, I. Komaromi, R. L. Martin, D. J. Fox, T. Keith, M. A. Al-Laham, C. Y. Peng, A. Nanayakkara, M. Challacombe, P. M. W. Gill, B. Johnson, W. Chen, M. W. Wong, C. Gonzalez, and J. A. Pople, Gaussian, Inc., Wallingford CT, 2004.

[24] Becket, C.W.; *J. Am. Chem. Soc.*, **1947**, *69*, 2488-2495.

[25] Aston, J.G.; Szasa, G.J.; Fink, H.L.,; *J. Am. Chem. Soc.*, **1943**, *65*, 1135-1139.

[26] Merenyi, G.; Lind, J.; *Chem. Res. Toxicol.*, **1997**, *10*, 1216-1220.

[27] Grimme, S. *J. Comp. Chem.* **2004**, *25*, 1463.

[28] Grimme, S. *J. Comp. Chem.* **2006**, *27*, 1787.

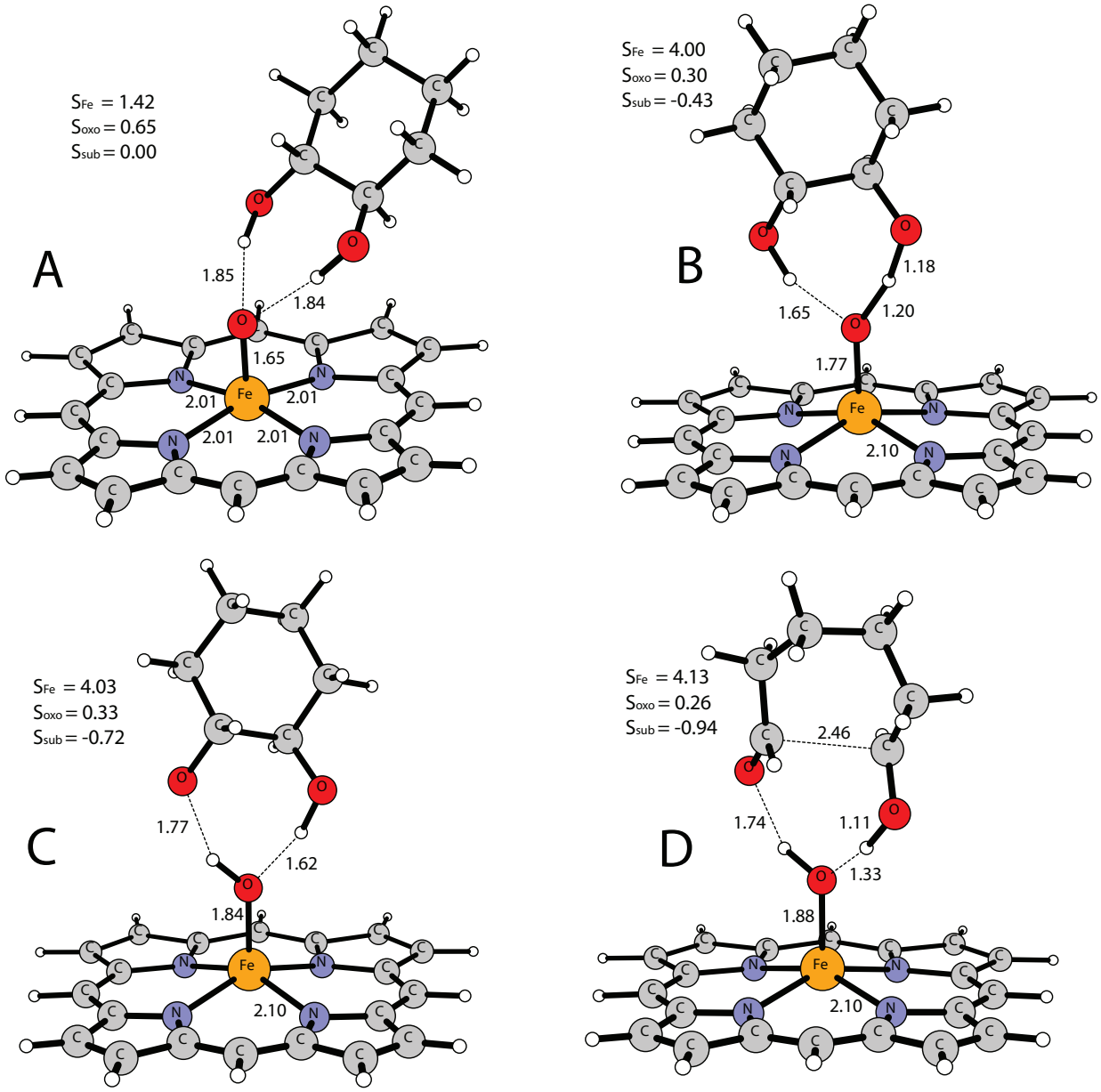

Figure 7: Optimized structures of **A**: the reactant complex [(Porph)Fe(IV)(O)(C_6H_{10}(OH)$_2$)] in its ground triplet state; **B**: HAT transition state in AFM quintet state; **C**: AFM quintet state for the intermediate complex [(Porph)Fe(III)(OH)(C_6H_{10}(OH)O$^\bullet$)]; **D**: transition state for the second HAT and C-C bond cleavage. The most important distances and spin populations are given.

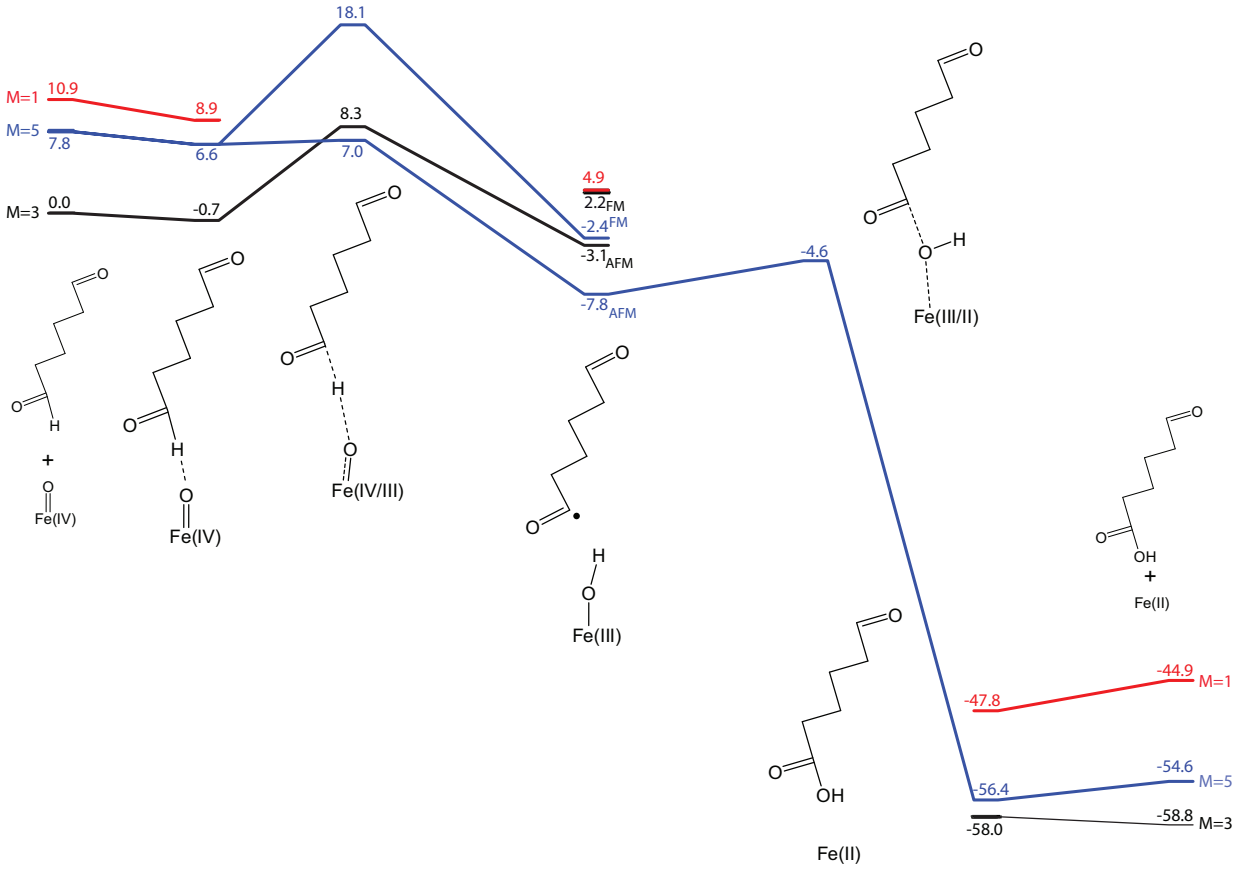

Figure 8: Energy diagram for the oxidation of the first carbonyl group of the adipic aldehyde.

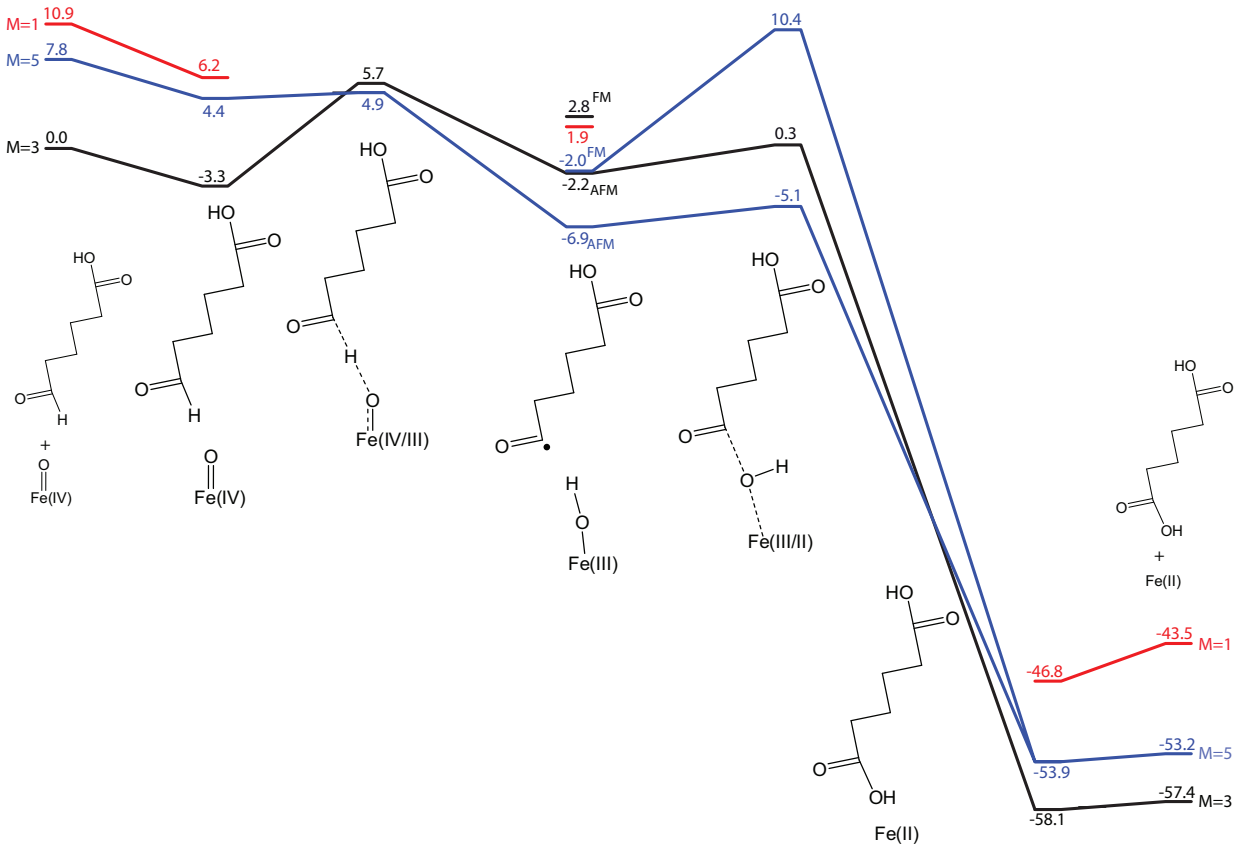

Figure 9: Energy diagram for the final oxidative step leading to adipic acid.

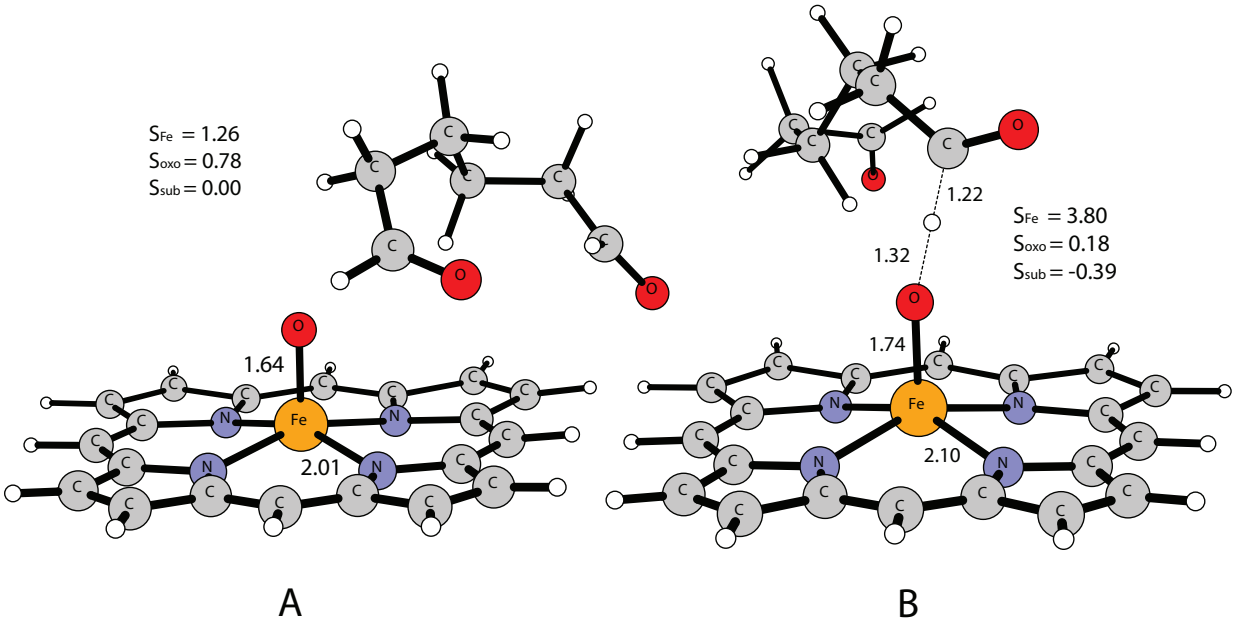

Figure 10: Optimized structures of **A**: the reactant complex [(Porph)Fe(IV)(O)($OHCC_4H_8CHO$)] in its ground triplet state; **B**: HAT transition state in AFM quintet state. The most important distances and spin populations are given.

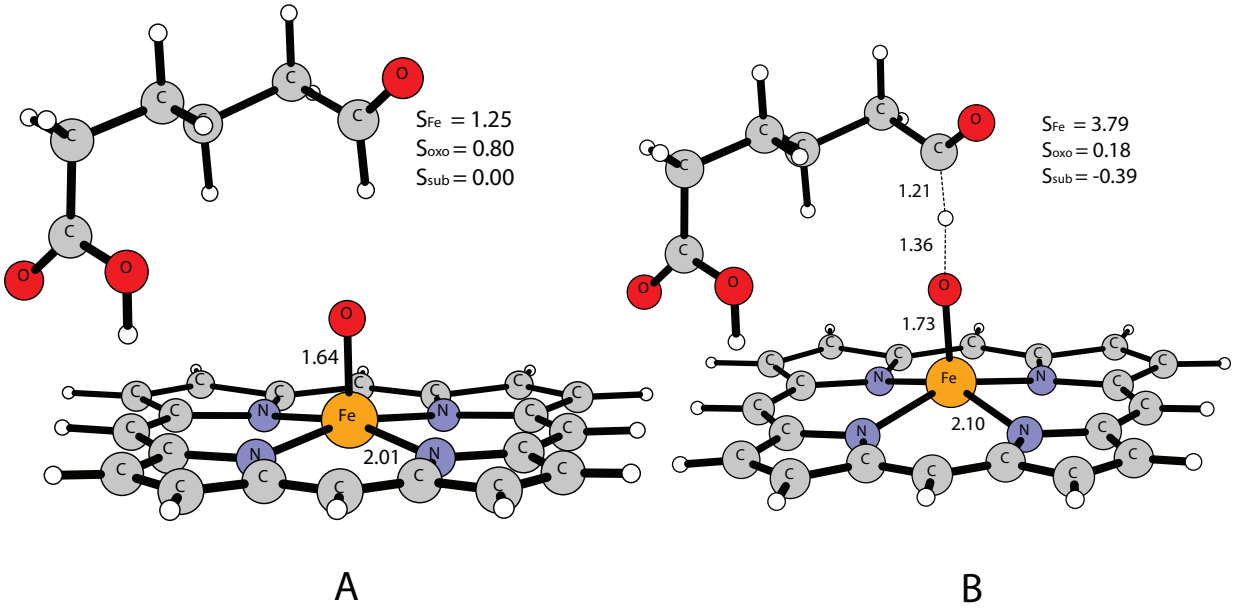

Figure 11: Optimized structures of **A**: the reactant complex [(Porph)Fe(IV)(O)($OHCC_4H_8COOH$)] in its ground triplet state; **B**: HAT transition state in AFM quintet state. The most important distances and spin populations are given.